JOURNAL OF CATALYSIS **170,** 108–122 (1997)
ARTICLE NO. CA971713

Characterization and Hydrodesulfurization Activity of W-Based Catalysts Supported on Al_2O_3–TiO_2 Mixed Oxides

J. Ramírez and A. Gutiérrez-Alejandre

UNICAT, Departamento de Ingeniería Química, Facultad de Química, UNAM, Cd. Universitaria, México D.F. 04510, México

Received September 5, 1996; revised April 1, 1997; accepted April 2, 1997

Characterization and catalytic activity of tungsten-based hydrotreating catalysts supported on $Al_2O_3(1-x)$–$TiO_2(x)$ mixed oxides ($x = 0.0$, 0.1, 0.5, 0.7, 0.95, and 1.0) have been obtained. The supports were characterized by X-ray diffraction (XRD), X-ray photoelectron spectroscopy, and FT-Raman spectroscopy. The catalysts in their oxided state were characterized by surface area, XRD, UV–Vis diffuse reflectance, FT-Raman spectroscopy, and temperature-programmed reduction (TPR). The catalysts in their sulfided form were characterized by FTIR spectroscopy and high-resolution electron microscopy. The catalytic activity of the different catalysts was evaluated in the thiophene hydrodesulfurization reaction at atmospheric pressure. The results indicate that the support composition and properties determine the type of tungsten species present on the surface. The tetrahedral tungsten species present on the alumina support change gradually to different octahedral species as the contents of titania in the support is increased. The presence of titania in the support leads to oxotungstate species with greater lateral interaction than in the case of the pure alumina-supported catalyst. These changes in the type of tungsten species are accompanied by changes in the reducibility and number of species detected by TPR. From the characterization results a picture of the structural changes in the tungsten species as the titania content in the support is increased is proposed. The changes in the catalytic activity trend with titania content can be rationalized in terms of the changes in the dispersion and morphology of the WS_2 crystallites, which are in turn related to the type of tungsten species in the oxidic precursors, and also, in the rich titania catalysts ($x = 0.95$, 1.0), to the effect that a sulfided and/or reduced layer of titania appears to have on the reaction mechanism leading to much higher activities than those expected from purely structural changes of the tungsten species.

INTRODUCTION

Over the past years, Mo- and W-based catalysts supported on alumina have been widely used in hydrotreatment processes. Of these two catalytic systems, the one based on tungsten has been the least studied. Also, for these catalytic systems it is now well known that the type of support plays an important role and that their activity may be improved by the use of an adequate support (1). In the case of the tungsten-based catalysts, the effect of the support is of great interest since it has been clearly established (2–6) that in the preparation of these catalysts using the conventional alumina support, during the calcination step, a very strong interaction between the tungsten-oxided species and the alumina is developed. This strong interaction precludes the adequate sulfidation of the catalyst (7, 8) leading therefore to poor activity. It has been demonstrated that treatment of these catalysts at 673 K for 4 h in a sulfiding mixture of H_2/H_2S (15% v/v) achieves only about 70% sulfidation, whereas complete sulfidation is obtained with molybdenum-based catalysts under the same conditions (8).

In the attempts to overcome this difficulty researchers in the field have tried, either the modification of the alumina support or the use of other less interacting supports (1, 9–11). Among the supports studied, titania seems an interesting option in view of the high activity results obtained previously on Mo/TiO_2 systems (1). However, the titania supports present the disadvantage of a low surface area ($Sg \approx 50\ m^2/g$) and poor thermal stability compared to their alumina counterparts ($Sg \approx 200\ m^2/g$).

The use of alumina–titania-mixed oxides supports seems a good alternative to overcome the problems of the poor sulfidation shown by the alumina-supported catalysts and the low surface area of those supported on titania (11).

As for the characterization of the WO_3/Al_2O_3 catalysts, not as many studies as for the Mo system have been made. However, tungsten-based alumina-supported catalysts, although less studied than their molybdenum counterparts, have been characterized by means of different techniques such as Raman spectroscopy, UV–Vis diffuse reflectance spectroscopy (DRS), X-ray photoelectron spectroscopy (XPS), X-ray diffraction, and others (4, 6, 12–21). In spite of these efforts, there is still some controversy on whether the tungsten is in tetra or octahedral coordination on the surface of the alumina (4, 12). The reports from the literature indicate that the structure and dispersion of the oxidic tungsten phases present in the alumina supported catalysts, depend on the tungsten load and on the calcination temperature (4, 5, 12, 13, 22–27). Also, it has been reported that on

0021-9517/97 $25.00

alumina supported tungsten catalysts the reduction of the W^{6+} species takes place in a single step to W^0 (17, 28).

Regarding the studies of tungsten supported on titania, only a few studies have been reported (17, 26–29, 30, 31). Temperature-programmed reduction studies (17, 28) show that in these catalysts, in contrast with their alumina supported counterparts, the reduction of the WO_3 species occurs in two steps ($W^{6+} \rightarrow W^{4+} \rightarrow W^0$). During this process, the titania anatase phase is transformed to rutile although it has been found that this transition is inhibited by the presence of the tungsten species (29). It has been also found that at low tungsten loading (~6 wt% WO_3), wolframyl species in interaction with the support are present (29).

In a work by Hilbrig *et al.* (27), on the characterization of WO_3/TiO_2 catalysts by EXAFS and XANES, they proposed a structural model in which islands of surface tungstate species are formed by branched chains of WO_5 units with terminal WO_4 units anchored onto the titania surface via W–O–Ti bonds. In this structure, the adsorption of one or two water molecules increases the oxygen coordination to six for all the tungsten surface sites. They also concluded that the length of these chains, and thus the WO_4/WO_5 ratio, is determined by the degree of tungsten oxide surface coverage. In a recent work by Kim *et al.* (32) a series of supported tungsten oxide catalysts on different supports were structurally characterized by *in situ* Raman spectroscopy. In this work they proposed that the surface tungsten oxide species on Al_2O_3 and TiO_2 at high surface coverage possess a highly distorted, octahedrally coordinated surface tungsten oxide structure with one short W=O bond (mono-oxo species), while at low surface coverage an isolated, tetrahedral coordinated surface tungsten oxide species is present. In another work by Wachs (33) under ambient conditions, and where the surface was hydrated, their results showed that the molecular structures of the surface metal oxide species were determined by the net pH at the PZC (point of zero charge) of the supported metal oxide system.

To date there have been no reports on the characterization and HDS activity of tungsten-based catalysts supported on Al_2O_3–TiO_2 mixed oxides. It seems interesting then to study the changes that occur in the tungsten oxidic precursors as the nature of the support changes from alumina to titania passing through Al_2O_3–TiO_2 mixed-oxide supports, with variable amounts of titania, and the relationship between the type of tungsten surface species with the catalytic activity in HDS reaction. It is therefore, the object of the present work to characterize the oxidic precursors by different techniques (nitrogen physisorption, XRD, TPR, XPS, Raman spectroscopy, and DRS), and the sulfided catalysts (HREM and FTIR) obtained with a series of tungsten catalysts suppported on mixed Al_2O_3–TiO_2 supports with variable amounts of TiO_2 going from pure Al_2O_3 to pure TiO_2 and relate the results from these characterizations to the changes in catalytic activity observed in the thiophene hydrodesulfurization, which was used as a model reaction.

EXPERIMENTAL

Supports and Catalysts Preparation

A series of tungsten-based catalysts supported on Al_2O_3–TiO_2 mixed oxides with variable amounts of TiO_2, expressed as the molar ratio $x = TiO_2/(TiO_2 + Al_2O_3)$ ($x =$ 0, 0.1, 0.5, 0.7, 0.95, 1.0), have been prepared. The supports were prepared by the coprecipitation of titanium and aluminum isopropoxides following the same method described previously (11). Aluminum isopropoxide was dissolved in *n*-propanol (150 ml per gram of isopropoxide) under vigorous stirring. The required amount of titanium isopropoxide was added to this solution and the coprecipitation of the corresponding hydroxides was achieved by slowly adding to the above solution an amount of demineralized water equivalent to 33 times the required stoichiometric amount. The precipitate was left under slow agitation for 24 h and then was filtered and washed five times with water in an amount of 250 ml per gram of product each time. Later on, the solid was dried at 373 K for 24 h and calcined at 773 K for 24 h. The solids prepared were named Al–Ti(x), where x is the molar ratio $TiO_2/(TiO_2 + Al_2O_3)$.

A series of W catalysts containing 2.8 atoms of W per square nanometer of support surface were prepared by impregnating the above supports (pore volume method), using the appropriate amounts of an aqueous solution of ammonium metatungstate ($(NH_4)_6H_2W_{12}O_{40}$). The impregnated samples were dried at 373 K for 12 h and later calcined at 773 K for 3 h; hereafter the catalysts will be referred as W/Al–Ti(x).

Supports and Catalyst Characterization

The specific surface areas of the samples were obtained by nitrogen physisorption in an automated BET apparatus. X-ray diffraction of the supports and catalysts were obtained in a Siemens D-500 diffractometer using the Cu $K\alpha$ radiation ($\lambda = 1.5418$). XPS measurements were performed in a Perkin–Elmer spectrometer using monochromatic Al $K\alpha$ radiation. The C1*s* binding energy of spurious carbon (BE = 284.5 eV) was taken as reference. The Raman spectra were recorded on a Nicolet 950 FT-Raman spectrometer equipped with a InGaAs detector and a Nd : YAG laser source, in the frequency zone 50–3500 cm^{-1}. The spectral slit width was typically 4 cm^{-1}. In all the spectra shown here, the contribution of the support has been subtracted in order to minimize the fluorescence effect present in the alumina support. UV–Vis diffuse reflectance spectra in the wavelength region 250–2500 nm were obtained in a Cary 5 E UV–Vis–NIR spectrometer using $BaSO_4$ as reference for the supports and the support itself as reference for the catalysts. Temperature-programmed reduction (TPR) measurements were performed in a flow apparatus with an argon–hydrogen (70% Ar v/v) mixture as reducing gas and a thermal conductivity detector. The gas mixture flow was 25 ml/min and the heating rate of the samples was 10 K/min. Samples of 0.25 g were used in each measurement. Before TPR, the samples were pretreated in air at 773 K for 2 h. Hydrogen consumption was evaluated using as a standard reference the reduction of V_2O_5, as previously reported (34). The infrared spectra of the oxided state of the samples were recorded in the 4000–200 cm^{-1} range on a Nicolet 510 FT-IR spectrometer working at a resolution of 4 cm^{-1} and with 400 scans. These samples were recorded using KBr wafers. Compensation of support absorption was used by subtraction of a spectrum of an equivalent amount of support from the spectra of the samples.

Catalytic Activity

Before the activity tests, the catalysts were sulfided under a H_2/H_2S 15% (v/v) gas mixture for 4 h at 673 K. After that, measurement of catalytic activity was conducted in a typical microreactor apparatus. Hydrogen was bubbled through a saturator filled with thiophene, maintained at 273 K. The gas mixture was passed through a heated Pyrex reactor with temperature regulation operating at atmospheric pressure which contained 0.1 g of catalyst. Reactants and products analysis were performed by on-line gas chromatography. All the catalytic activities reported here are steady-state values reached after the catalyst had been stabilized 12 h. Activity measurements were obtained at 603 K. The experiments were performed at low conversions, below 15% and rates of reaction were calculated as $R = (Q/W)X$, where R is the specific rate (moles of thiophene transformed per second per gram of catalyst, Q is the molar flow of reactant per second, W is the mass of catalyst in grams, and X is the fractional thiophene conversion, defined as moles of thiophene converted per mole of thiophene in the feed.

TABLE 1

Surface Area S_{BET} (m^2/g) and Catalytic Activities of the W/Al_2O_3–$TiO_2(x)$ Catalysts in the Thiophene HDS Reaction

$x = TiO_2/(Al_2O_3 + TiO_2)$	0.0	0.1	0.5	0.7	0.95	1.0
S_{BET}	205	196	188	162	68	10
R_1	2.53	4.81	5.85	7.20	7.62	29.7
R_2	0.52	0.94	1.10	1.17	0.56	0.30

Note. $R_1 = (mol/s/m^2) \times 10^{10}$; $R_2 = (mol/s/g) \times 10^7$.

RESULTS

Surface Area

The results from the surface area measurements are shown in Table 1 for each catalyst composition. It may be observed from this table that the surface area of the catalysts presents only a slight drop between the samples with $x = 0$ (Sg = 205 m^2/g) and $x = 0.5$ (Sg = 188 m^2/g), to later descend in a more pronounced way between $x = 0.7$ (Sg = 162 m^2/g) and $x = 1.0$ (Sg = 10 m^2/g). All the catalysts showed a monomodal pore size distribution curve, which gave an indication of the absence of important segregation of the different oxide supports in the catalysts formulations.

X-Ray Diffraction (XRD)

The diffractograms of the catalysts taken in the range $2\theta = 19$–90 are shown in Fig. 1. No diffraction lines of any tungsten phase were detected in the different samples and the only peaks present in the diffractograms corresponded to the γ-Al_2O_3 phase (W/Al–Ti($x = 0.0$, 0.1) catalysts) or the anatase phase (W/Al–Ti($x = 0.95$, 1.0) catalysts). In the W/Al–Ti(1.0) sample some traces of poorly crystallized rutile were also observed. With respect to the samples with $x = 0.5$ and $x = 0.7$, the diffractograms show a completely

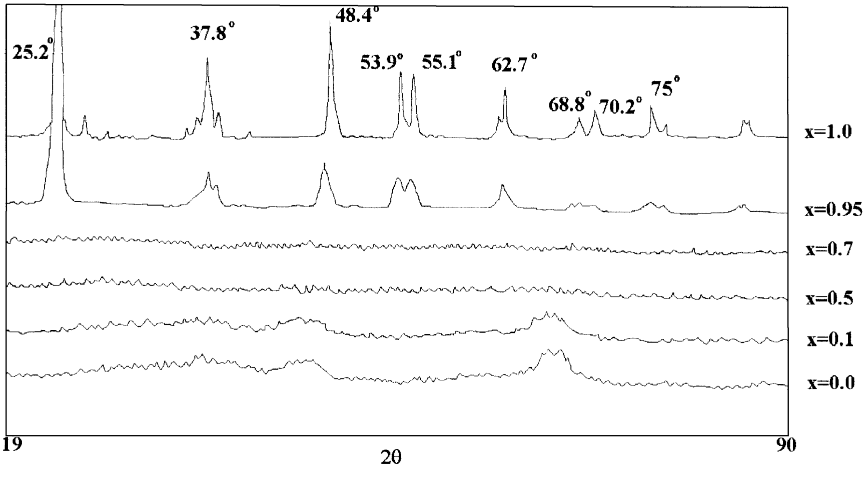

FIG. 1. X-ray diffractograms of the W/Al–Ti(x) catalysts.

amorphous system. The above observations indicate that at this measuring scale, the tungsten phases were well dispersed on the different supports forming either an amorphous phase or microcrystallites of less than 4.0 nm in size.

UV–Vis (DRS)

According to the literature (35), the bands corresponding to octahedral (Oh) and tetrahedral (Td) tungsten geometry appear in the spectral region of 250–280 nm. The maxima of the bands have been reported in 250 nm for octahedral tungsten, in 340 nm for WO_3 which also contains tungsten in octahedral coordination, and in 275 nm for tetrahedral tungsten species in $Al_2(WO_4)_3$.

The electronic spectra of the W/Al–Ti(x) catalysts, using the corresponding support as reference, are shown in Fig. 2. As can be observed in Fig. 2, for the W/Al–Ti(0.0) catalyst only an intense single band is present in the region of the spectrum where the contributions from tungsten W^{6+} in tetrahedral coordination appear. As the content of TiO_2 in the support is increased, the intensity of the bands decrease and the maximum shifts to higher wavelength.

The maximum in the most intense absorption band of the W/Al–Ti(0.1) catalyst appears in 306 nm and does not correspond to either tetrahedral ($\lambda = 275$ nm) or octahedral ($\lambda = 340$ nm) well-defined tungsten species. A shoulder in this band is also present in the spectrum of this catalysts in the region 350–390 nm which has been assigned to the presence of octahedral tungsten in WO_3 (30).

As the contents of TiO_2 is increased further, only a single band in the region of octahedral tungsten species ($\lambda = 350$–390 nm) was evident. The decrease in the relative intensity of this band as the titanium content is increased is probably due to the drop in specific area of the titanium rich catalysts, which is accompanied by the corresponding drop in the amount of tungsten per gram of catalyst.

The change observed in the intensity of the tungsten band ($\lambda = 250$–400 nm) for the samples with $x = 0$ to $x = 0.5$, which have approximately the same specific surface area, also indicates a shift from tetrahedral to octahedral coordination since normally the octahedral bands are much less intense than tetrahedral ones.

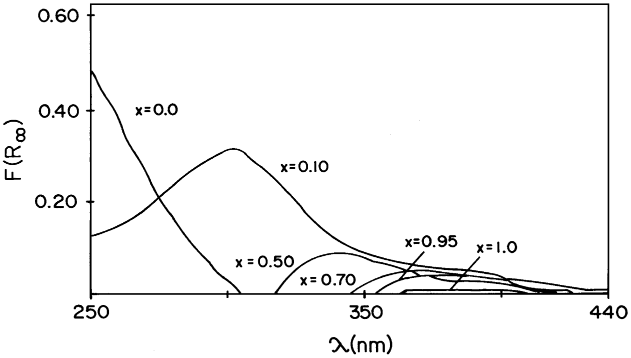

FIG. 2. Diffuse reflectance electronic spectra of the W/Al–Ti(x) catalysts.

TABLE 2

XPS Results for Al–Ti(x) Supports

x	(Ti/Al)XPS	(Ti/Al)theoretical	Binding energies (eV)[a]		
			Ti2p	Al2p	O1s
0.0	0	0	—	74.1	530.1
0.1	0.050	0.055	457.8	73.7	530.1
0.5	0.413	0.500	458.3	74.2	530.1
0.7	0.840	1.166	458.3	74.2	529.9
0.95	3.647	9.500	458.6	74.3	529.8
1.0	—	—	458.7	—	529.9

[a] The C1s binding energy (BE = 284.5 eV) was taken as reference.

As interesting fact that should be noted here is that having the W^{6+} a d^0 electronic configuration it should not show any d–d transition bands. The bands previously observed in the literature and in the present work most probably are due to charge transfers which induce a slightly reduced state in the tungsten.

It appears then from the above observations that the incorporation of TiO_2 to the catalyst support leads to a higher population of octahedral tungsten species and in the titanium rich samples mainly tungsten in octahedral coordination seems to be present.

X-Ray Photoelectron Spectroscopy

Table 2 shows the experimental (XPS) and theoretical results of the Ti/Al atomic surface ratio for the Al–Ti(x) support samples. In Table 2, it can be observed that the Ti/Al ratio increases almost linearly from the Al–Ti(0.0) to the Al–Ti(0.5) support sample, to later increase more slowly in the titanium rich samples ($x = 0.7$ and 0.95). This behavior could be due to an agglomeration of TiO_2 on the surface leading therefore to a depart from linearity in the XPS Ti signal. With respect to the binding energies (BE) of the aluminum and titanium elements, also given in Table 2, they are reported in the literature (36) at 74.10 and 458.5 eV, respectively. These values are in good agreement with the ones obtained in this work for the pure oxide samples ($x = 0$ and 1.0). In case of mixed oxide supports, a small shift in the BE of the Ti2p electrons from the Al–Ti(0.1) (457.8 eV), to the Al–Ti(1.0) support (458.7 eV) was observed, this shift toward higher BE indicates a change in the Ti^{4+} ions surroundings.

FT-Raman Spectroscopy

The FT-Raman experiments are useful to inquire on the structural characteristics of supports and catalysts.

Supports. The titanium oxide presents two main distinct crystallographic structures: anatase and rutile. According to

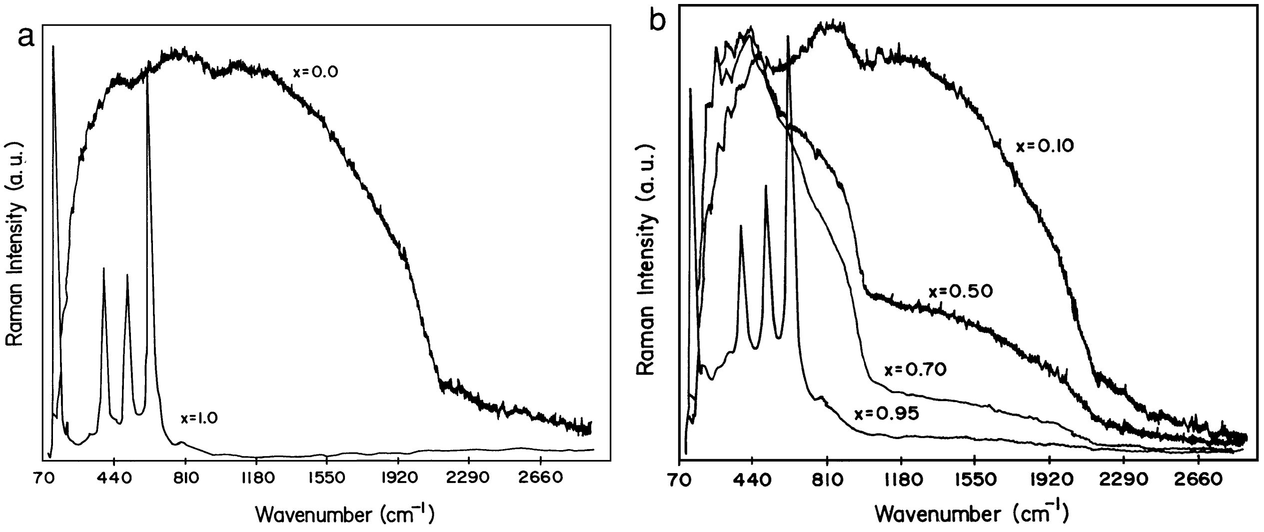

FIG. 3. (a) FT-Raman spectra of the pure alumina ($x = 0$) and pure titania ($x = 1.0$) supports. (b) FT-Raman spectra of Al–Ti(x) mixed-oxide supports.

literature reports (26, 37–39) Raman active bands for the anatase appear at 144, 199, 399, 520, 643, and 798 cm^{-1}, and for rutile at 144, 448, and 611 cm^{-1}. The γ-alumina support, on the contrary, has been reported to have no Raman active modes (5).

The Raman spectra of the Al–Ti(x) supports are presented in Figs. 3a and 3b. In Fig. 3a, where the spectra corresponding to the pure oxides are presented, it can be observed that the alumina support presents the phenomenon of fluorescence which has been previously reported by others (5). For the pure titania support Raman bands with maxima in 144, 196, 396, 520, 636, and 798 cm^{-1}, corresponding to the different vibrational Raman active modes of anatase are observed. Also, a small shoulder present at 441 cm^{-1}, and which may be assigned to the presence of small amounts of rutile (37) is present in this sample. In Fig. 3b where the Raman spectra of the mixed oxides is presented it is possible to see that the fluorescence effect due to alumina diminishes with the titania loading. It is evident that only at the high titania loading the fluorescence effect disappears indicating a full coverage of the alumina surface by the titania.

Catalysts. A further insight about the structural changes of the different tungsten phases present in the catalysts, as the titanium loading was varied, was obtained by FT-Raman. The results from this technique point out the existence of various tungsten species in the catalyst oxidic precursors. According to the literature, characteristic bands of tungsten oxidic phases appear at ~973 cm^{-1} and in ~853 cm^{-1} for the symmetric and antisymmetric vibrational modes of terminal W=O bonds in two-dimensional tungsten oxide species in interaction with the support. The characteristic vibrational modes of WO_3 have been reported at 805, 706, and 273 cm^{-1} (16). The bands corresponding to $Al_2(WO_4)_3$ typically appear at 1046–1057, 386, and 371 cm^{-1}. However, the precise identification of all the different modes of bond vibration of the tungsten species is obscured by the presence of TiO_2 strong bands which appear below 700 cm^{-1}.

The Raman spectra of the W/Al–Ti(x) catalysts taken at ambient conditions, after subtraction of the support spectra, are shown in Fig. 4. According to the literature (26), the

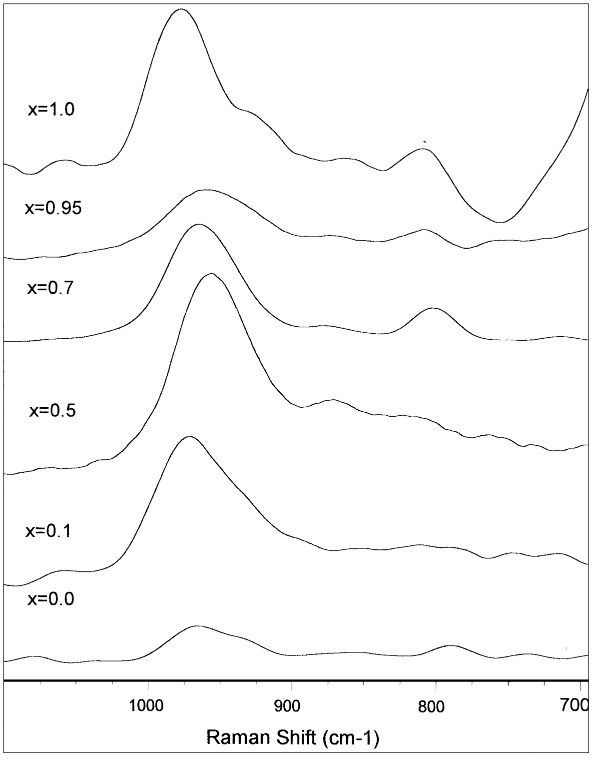

FIG. 4. FT-Raman spectra of W/Al–Ti(x) catalysts.

band with a maximum in 967 cm^{-1}, and which is present in all the catalyst formulations, has been assigned to the symmetric stretching vibration mode of W=O bonding in two-dimensional oxotungstate species in interaction with the support, which may be in tetrahedral or octahedral coordination depending on the surface tungsten loading and also on the level of hydration. As the content of titanium in the support is increased this band (~967 cm^{-1}) shifts toward higher frequencies, indicating different degrees of distortion. A similar shift has been reported, for catalysts supported on alumina and on titania (26, 37), as due to differences in the degree of hydration of the tungsten species and also as a consequence of a greater lateral interaction which affects the hydration and distortion of the oxotungsten species. In our samples, since the Raman spectra were recorded under ambient conditions a certain degree of hydration is expected.

The spectra also show the appearance of a band in 803 cm^{-1} which is more evident in the catalysts with high titania content ($x = 0.7$, 0.95, and 1.0). This band has been reported in previous works as due to crystalline WO_3 (5). However, since the 803 cm^{-1} band in our spectra was rather weak, one should be careful not to confuse it with an also weak band due to the presence of anatase at (~798 cm^{-1}) corresponding to an overtone of the anatase band at 396 cm^{-1}. This question will be addressed later on in the discussion of results.

The small band appearing in the region of 840–880 cm^{-1} has been assigned to the asymmetric mode of a W–O–W linkage which has been mentioned to correspond to a surface polytungsten oxide species on the surface of the support oxide (30).

Temperature-Programmed Reduction

In order to inquire about the number, nature, and reducibility of the tungsten species present in the catalyst oxidic precursors, temperature-programmed reduction experiments were performed with the supports and catalysts.

Supports. Figure 5 presents the TPR thermograms of the different supports. In Fig. 5, one observes, in agreement with previous reports (17), that no reduction takes place in the pure alumina sample. Also, in the Al–Ti(0.1) sample, no clear peak of reduction was evident although a small hydrogen consumption was detected at the high temperatures. On the other hand, in the Al–Ti(0.5) sample an intense broad peak of reduction with a maximum at 1073 K was clearly evident. This peak presented a shoulder around 853 K and in the high-temperature range ($T > 1173$ K). It was also clear in this sample the beginning of the reduction of another species with $T_{max} > 1273$ K.

For the Al–Ti(0.7) support, the shoulder present in the previous sample at about 853 K developed into a clear peak and the peak which in the Al–Ti(0.5) sample appeared at $T_{max} = 1073$ K shifted to lower temperatures and appeared at $T_{max} = 1008$ K in the Al–Ti(0.7) sample. In this sample there was also evident the reduction of a high-temperature species with $T_{max} > 1173$ K. In the samples with the highest titanium content (Al–Ti(0.95, 1.0)), the detection of the reduction peaks was more difficult due to the low tungsten loading per gram of catalyst which was a consequence of their lower surface area. Nevertheless, a low reduction temperature peak ($T_{max} \sim 837$ K), and the beginning of the high-reduction temperature peak ($T_{max} > 1173$ K) were evident in both supports. The peak which reduction took place at intermediate temperatures and which T_{max} of reduction shifted from 1073 to 1008 K seems to be due to the reduction of titanium species with different degrees of interaction with the alumina.

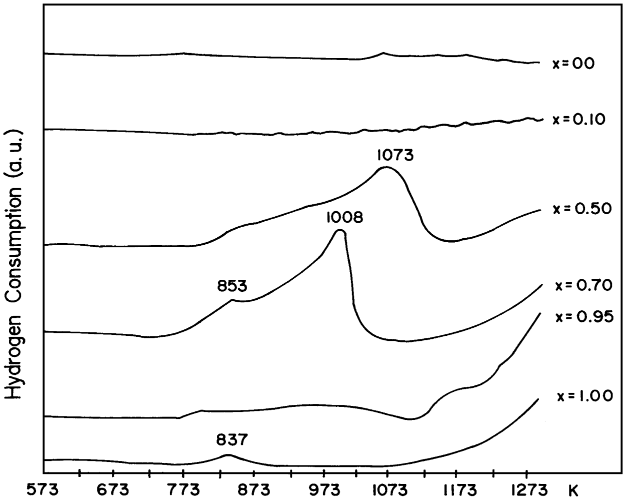

FIG. 5. TPR thermograms of Al–Ti(x) supports.

The results from the titania pure sample indicate in agreement with previous reports (17), that the low reduction temperature peak ($T_{max} = 837$ K) is due to the reduction of anatase. The high reduction temperature peak ($T_{max} > 1173$ K) is most probably due to the reduction of the rutile phase formed from anatase during the heating process since the transition temperature for the anatase to rutile transformation is about 1023 K.

The above results indicate that at low titanium loading a strong interaction exists between the titanium oxide species and the alumina matrix, whereas at higher titanium loading ($x > 0.5$), some segregation of anatase occurs, causing the appearance of low-temperature reduction peaks.

Catalysts. The W/Al–Ti(x) catalysts TPR profiles are shown in Fig. 6. Clearly, the analysis of Fig. 6 reveals that the W/Al–Ti(x) system is quite complex, however, taking into account the previous reports for the W/Al_2O_3 and the W/TiO_2 (17, 28) systems, and the results outlined above for the supports used here, the interpretation of the TPR profiles of the W/Al–Ti(x) system appears possible.

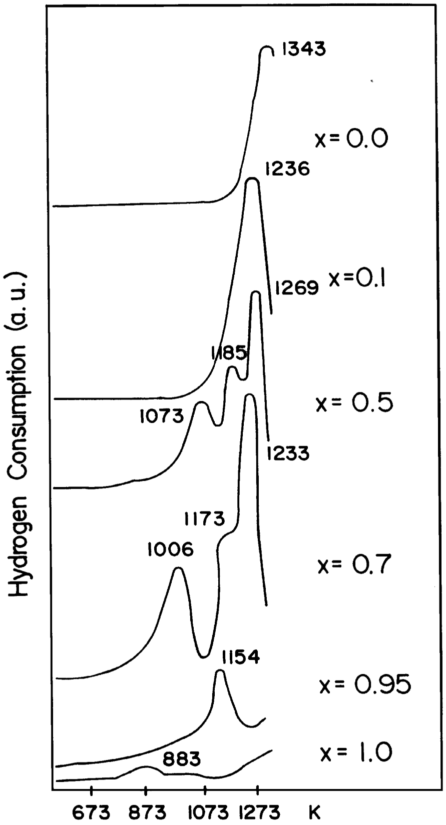

FIG. 6. TPR thermograms of W/Al–Ti(x) catalysts.

It has been reported previously using tungsten loading similar to that used in this study that the reduction of the tungsten oxide species supported on alumina presents only one high-temperature peak due to the reduction of tetrahedral tungsten species in strong interaction with the alumina support. The TPR profile of the W/Al–Ti(0) catalyst is clearly in agreement with those previous reports. As the content of titania is increased in the catalysts, the $T_{\max}$ of reduction of this peak shifts to lower temperatures and the appearance of another reduction peak, which is only a small shoulder in the W/Al–Ti(0.1) sample, but that develops into a clear peak with $T_{\max} = 1185$ and 1173 K in the W/Al–Ti(0.5) and W/Al–Ti(0.7) catalyst samples is observed.

In the W/Al–Ti(0.95) catalyst sample, only a broad reduction peak with $T_{\max} = 1154$ K is clearly evident. In this sample it is observed also the beginning of the reduction of a high reduction temperature species which, from the results obtained for the pure supports, seems to be due to the beginning of the reduction of rutile.

The results from the W/Al–Ti(1.0) sample did not allowed a clear interpretation due to the low intensity of the signals which were a result of the relatively low amount of tungsten in this sample. It must be remembered that all catalysts had a tungsten content of 2.8 W atoms/nm^2 and that the surface areas of the rich titanium samples ($x = 0.95$ and 1.0) are quite low compared to the other catalyst samples with less titanium. Also, in the study of TPR profiles of different catalysts it is not advisable to change the size of the sample since, as has been demonstrated before (40), the TPR results from samples of different size may not be comparable. However, in this sample (W/Al–Ti(1.0)), a small hydrogen consumption due to the reduction of the anatase present in the support was detected at about 893 K. Another even smaller hydrogen consumption peak, most probably due to the reduction of W^{6+} species appeared at about 1053 K and the beginning of the high reduction temperature peak, consistent with the reduction of rutile started to appear above 1173 K.

The above results confirm that the incorporation of titanium oxide to the catalyst support induces a change in the type of tungsten oxide species which is reflected in an easier reduction than in the pure alumina supported catalyst. It appears that as the titanium loading is increased, a higher population of easily reducible octahedral tungsten species is present in the catalysts.

High-Resolution Electron Microscopy (HREM)

After sulfidation, the catalysts were characterized by HREM. Electron microscopy is a helpful technique for obtaining evidence of the changes in the morphology, dispersion, and homogeneity of the supported metal sulfides. However, in the interpretation of the results, one must be aware of the limitations of the technique. Clearly, one of the limits of the limits of the technique comes from the difficulty in observing very small WS_2 particles of less than 1 nm in length. Also, during the observations, only the WS_2 platelets which have the c axis perpendicular to the incident beam will be observed. In our case, the fact that the same tungsten surface concentration was used in the preparation of all the catalysts diminished the effects induced by the changes in texture of the different catalyst supports. Nevertheless, it may be possible that some of the changes observed in the tungsten sulfide crystallites may not only be due to changes in the chemical nature of the support but also to changes in the texture of the support. With these precautions in mind we can then go through the analysis of the micrographs of the sulfided catalysts.

The micrographs of the catalysts (Figs. 7a and 7b) show the typical lattice fringes representing the basal plane of WS_2 structures with 6.18 Å interplanar distances (8, 41). These structures appear well dispersed in all the samples; however, changes in the stacking, length, and population were observed depending on the amount of titania in the catalyst support.

Measurement of length and number of layers of 300–400 WS_2 crystallites allowed us to estimate the overall changes in the relative dispersion in the different catalyst samples. Figures 8 and 9 show the percentage distribution plots for

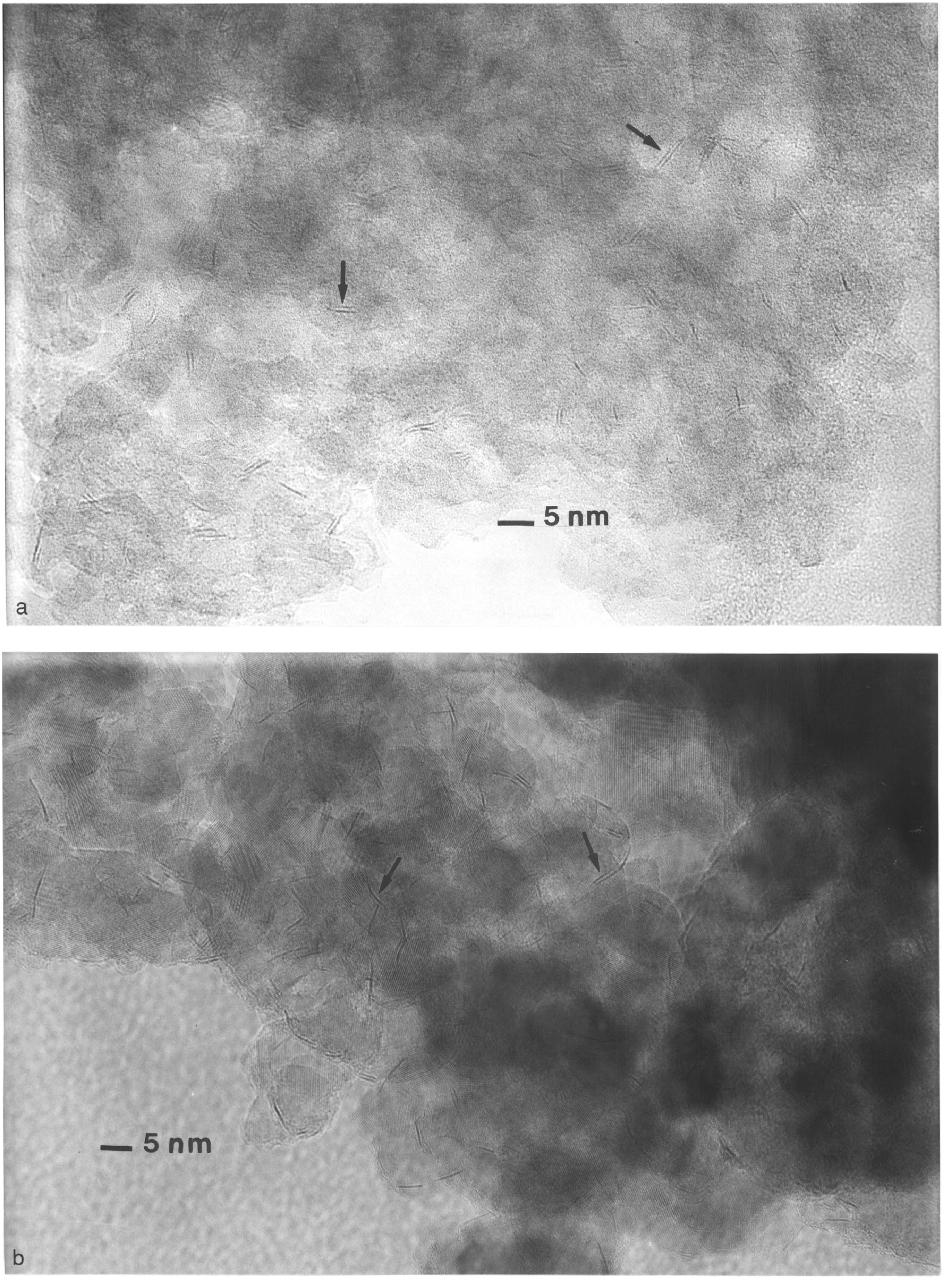

FIG. 7. (a) Typical micrograph of the W/Al–Ti(0) catalyst showing WS_2 crystallites. (b) Typical micrograph of the W/Al–Ti(0.95) catalyst showing WS_2 crystallites.

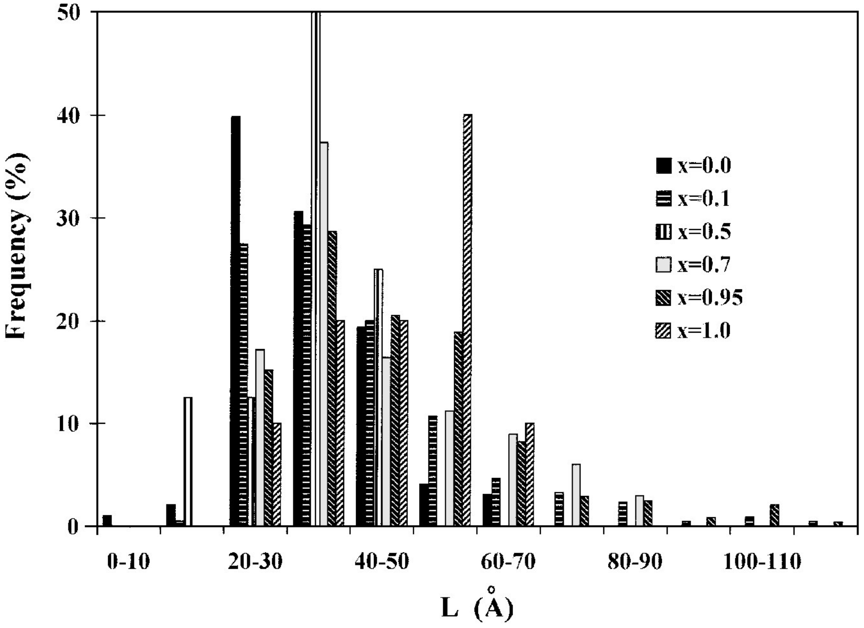

FIG. 8. WS_2 crystallite size distribution plot in the W/Al–Ti(*x*) sulfided catalysts.

the length (L) and number of layers (N), respectively, of the WS_2 structures found in the W/Al–Ti(*x*) catalyst series.

In Fig. 8 it is possible to see that for the W/Al–Ti(0.0) catalyst, the majority of the WS_2 crystallites have a length between 20 and 30 Å, whereas for the catalysts supported in the mixed oxides the main length is between 30 and 40 Å. Regarding the W/Al–Ti(1.0) catalyst, the maximum number of crystallites lies in 50–60 Å length. It appears then that the length of the WS_2 crystallites increases with the titanium loading. However, since partially sulfided tungsten is not clearly observed by this technique and it is well known that the tungsten oxide precursor is difficult to sulfide when supported on alumina, only about 40% at the sulfiding conditions of this work, the above results on the growth of the WS_2 crystallites with titania loading may be due to either a better sulfidation of the catalyst or a lateral growth of the crystallites resulting from the migration of the tungsten-sulfided species which becomes more important as the interaction with the support is diminished by the incorporation of titania into the catalyst support. As for the number of layers observed in the WS_2 crystallites, the results in Fig. 9 indicate that the presence of titania in the support induces a low stacking of the WS_2 crystallites. It should be considered that it may be possible that under reaction conditions the sulfided phase can sinter or be further sulfided. Therefore, the size and stacking of the WS_2 crystallites measured before reaction should be taken with due care. In our experiments we expect, due to the conditions of sulfidation, an incomplete sulfidation of the tungsten phase, especially in the catalysts supported on alumina-rich supports. Because of this, an attempt to correlate catalytic activity with the number of edge sites present on the catalyst was not made. Such an exercise is more suitable for Mo-based catalysts or for Ni-promoted tungsten catalysts where higher degrees of sulfidation are observed, as one of us has reported previously (42, 43).

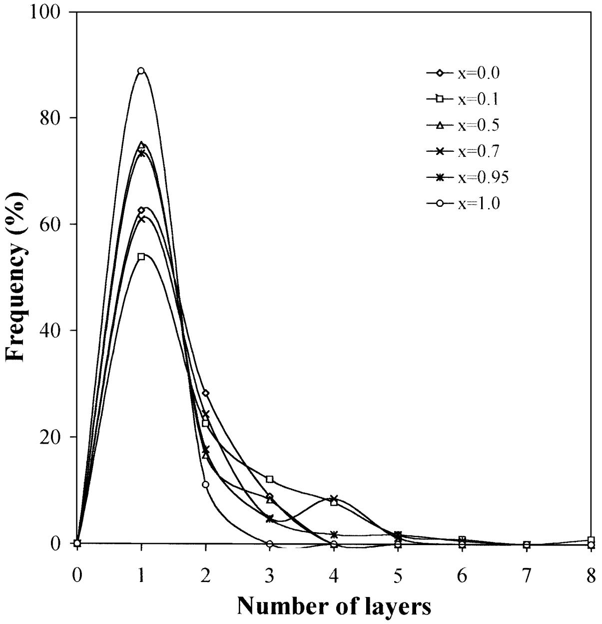

FIG. 9. Distribution plot of the number of layers in WS_2 crystallites.

Catalytic Activity

The catalytic activity of the sulfided form of the W/Al–Ti(*x*) catalysts was tested in the hydrodesulfurization of thiophene at atmospheric pressure. However, since the surface area of the different catalysts formulations varies between a wide range of values, comparison of the catalytic activities will be best made in terms of the reaction rates expressed as thiophene moles transformed per second and per square meter. Table 1 shows the activity of the catalysts at 603 K as the content of titania is varied. It can be observed in Table 1 that the maximum activity per gram of catalysts is observed for the W/Al–Ti(0.7) catalyst. However, this result can be easily explained since all the catalysts were prepared with the same tungsten surface concentration (2.8 W atoms/nm^2) and the specific surface area of the supports reached a maximum at $x = 0.7$. However, if one looks at the catalytic activities expressed per square meter, it is observed that the activity of the catalysts increases slightly and linearly with titanium loading from the catalyst supported on pure alumina ($x = 0.0$) to the catalysts with $x = 0.95$. The catalyst supported on pure titania, however, shows a sharp increase in catalytic activity. These differences in activity could be due to changes induced by the support in the dispersion of the tungsten-sulfided phase, to the level of sulfidation of the tungsten phases or to an effect caused during reaction by the presence of a partly reduced and/or sulfided titanium phase which could act as a promoter. Furthermore, these changes in catalytic activity must be also related to the structural changes of the tungsten phases, induced by the incorporation of titanium to the catalysts, in the oxided state catalyst precursors.

DISCUSSION

Supports

One of the interesting features of using the Al–Ti(x) mixed oxides as catalysts supports is that higher surface areas than those obtained in the pure oxides are obtained, even at high titanium loading. The results from the pore size distribution curves obtained for all the supports showed a homogeneous unimodal distribution of pore sizes indicating mainly the existence of a true microcomposite structure rather than a mixture of the individual materials.

The X-ray diffraction patterns of the supports indicate that, at this scale of observation, in the support samples with $x = 0$ to $x = 0.7$ the titanium is well dispersed. It is only in the titanium-rich samples ($x = 0.95$, 1.0) that bigger anatase crystals are detected. Also, a slight segregation of poorly crystallized titania in the form of rutile was detected in the samples with $x = 0.95$ and $x = 1.0$. Another interesting feature present in the support diffractograms is that the incorporation of titania appears to reduce the crystallinity of the γ-alumina phase present with respect to that in the pure alumina support. In fact the supports with $x = 0.5$ and $x = 0.7$ show a completely amorphous pattern.

The evolution of the FT-Raman spectra of the supports with titanium loading show that at $x = 0.95$ the surface of the support practically consists of titanium oxide (anatase) since at this titanium concentration practically no fluorescence originated by the alumina appears and only the characteristic anatase Raman bands at 144, 196, 396, 520, 636, and 798 cm^{-1} are clearly evident. This result is consistent with the XRD observations. The quantitative determination of the relative amounts of Ti and Al on the surface is beyond the scope of the present work.

In line with the above findings the distribution of titanium on the surface of the supports measured by XPS also showed that the Ti/Al atomic ratio increased linearly up to titania contents of $x = 0.5$ and then dropped slightly at $x = 0.7$ and more at $x = 0.95$. It appears that after the titania loading of $x = 0.5$, which also corresponds to the theoretical amount for the formation of aluminum titanate (Al_2TiO_5), some segregation of titania on the surface of the support takes place. The changes observed in the binding energy of titanium which changed from 458.7 eV in the pure titania sample to 457.8 eV in the Al–Ti(0.1) support, although small, indicate the possibility of the formation of Ti–O–Al bridges, since the influence of the Al^{3+} ions would cause a shift to lower binding energies in the titanium electrons. For the Al–Ti(0.95) rich titanium sample, the binding energy is the same as in the pure titania sample, indicating that important amounts of TiO_2 are present on the surface.

Catalysts

The tungsten addition to the supports produces only a small decrease in surface area indicating a uniform distribution of the tungsten oxide on the surface of the supports. Since the X-ray diffraction patterns of the different catalysts formulations did not show any diffraction lines different from those due to the Al–Ti(x) supports, the tungsten oxidic phase at this scale of observation seems to be well dispersed on the surface of the different supports.

With respect to the changes induced in the structure of the oxidic tungsten phases by the incorporation of titania in the support, the shifts observed in the DRS absorption bands, once the spectra of the support was subtracted from each sample (Fig. 2), indicate, at the level of tungsten loading used in this work, the preference of the W^{6+} ions for a tetrahedral coordination when supported on alumina. However, as the titanium loading increases, the shift in the absorption edge toward higher wavelengths indicates a reduction in the tetrahedral species and an increase in the octahedral ones which is more notorious at the high titania loading. It appears then that in the pure alumina support only tetrahedral species are present, at intermediate titania contents ($x = 0.1$–0.5) both tetrahedral and octahedral or highly distorted species are present, and at high titania contents mostly octahedral tungsten species are present. The decrease in the intensity of the DRS absorption bands with the titanium loading is also in line with the fact that the intensity of the octahedral bands is smaller than for tetrahedral ones. Furthermore, the absence of octahedral bands in the W/Al–Ti(0.0) catalysts is in line with the TPR results of this sample in which, also in agreement with the literature (17, 28), only the existence of a single reduction peak at 1343 K which has been assigned to tungsten species in tetrahedral coordination in strong interaction with the alumina support is observed (Fig. 6). When a small amount of titanium is incorporated to the alumina support (W/Al–Ti(0.1) sample), the observed shift in the $T_{\max}$ of reduction from 1343 to 1236 K indicates the presence of tungsten species with less interaction with the support than those present in the pure alumina supported sample. This effect is more clearly observed in the W/Al–Ti($x = 0.5, 0.7$) samples where a clear reduction peak develops at $T_{\max} = 1185$ K in the W/Al–Ti(0.5) sample and at $T_{\max} = 1173$ K in the W/Al–Ti(0.7) catalyst. In these two samples, in addition to the high-temperature reduction peak, we also observe the appearance of a peak with $T_{\max} = 1073$ K (W/Al–Ti(0.5) sample) and with $T_{\max} = 1006$ K (W/Al–Ti(0.7) sample), which are due to the reduction of the titania in the support (see Fig. 6), and also, possibly, to the reduction of some tungsten species in octahedral coordination. The reduction of W^{6+} species has been reported (17) to occur in tungsten catalysts supported on pure titania, in two stages, the first $W^{6+} \rightarrow W^{4+}$ at $T_{\max} = 1017$ K and the second, $W^{4+} \rightarrow W^0$, at $T_{\max} = 1248$ K. The appearance of this second reduction stage is due to the stabilization of the W^{4+} oxidation state by the titania.

As mentioned previously, the titanium rich samples (W/Al–Ti($x = 0.95, 1.0$)) due to their the small surface area and therefore low amount of tungsten per gram of catalyst, do not lend themselves to a clear interpretation. Nevertheless, in these samples in which the support surface is practically titania, the presence of tetrahedral tungsten, if it existed, would be only minor and could be confused with the start of the reduction of the rutile species formed during the TPR processes.

The reduction peak that in the W/Al–Ti(0.95) sample which appears at $T_{\max} = 1154$ K has been assigned to tungsten species, possibly WO_3. Salvati *et al.* (4) have also reported the reduction of tungsten species at $T_{\max} = 1150$ K in NiW/Al_2O_3 catalysts; however, they do not state clearly the nature of this tungsten species. The broad small reduction peak observed in the W/Al–Ti(1.0) sample cannot be clearly interpreted.

According to the above results, the increase of titanium in the catalyst support produces a change in the distribution of tungsten species, leading to species with less interaction with the support which are more easily reduced. This last statement is confirmed by the total hydrogen consumption results and by the degree of reducibility estimated assuming that only the tungsten is reduced during the process (see Table 3). This assumption is clearly not accurate since part of the titania in the support is also reduced. It is for this reason that the degree of reducibility estimated under the above assumption leads to values higher than 100% in the pure titania supported sample. Although it is not possible to separate in an accurate way the contributions of tungsten and titanium reduction to the total hydrogen consumption, it is clear that the incorporation of small amounts of titanium lead to a sharp increase in the consumption of hydrogen and therefore in the degree of reducibility. Since this trend does not continue from $x = 0.1$ to $x = 0.7$ one may reasonable assume that great part of the increase in the hydrogen consumption with titanium loading in these samples ($x = 0.1, 0.5, 0.7$) is due to the increased reduction of the tungsten species rather than to titanium reduction. It is interesting to note that the trend of the degree of reducibility with the titanium loading follows the same shape as the catalytic intrinsic activity versus titanium content (see Fig. 10 and Table 1). Clearly, the variations in the degree of reducibility of the catalysts and their catalytic activity will be related to the type of tungsten species present in the oxided catalyst precursors.

TABLE 3

Total Hydrogen Consumption (HC) and Degree of Reducibility[a] for W/Al–Ti(x) Catalysts

x	0.0	0.10	0.50	0.70	0.95	1.00
HC (mmol of H_2/m^2) $\times 10^4$	9.93	17.01	19.45	17.34	30.47	56.30
Reducibility (%)	33.2	60.0	68.5	66.6	94.8	164.0

[a] Calculated assuming that only W is reduced ($W^{6+} \rightarrow W^0$).

The results from the Raman analysis of the oxidic catalyst samples confirm the existence of various tungsten species in the catalyst precursors. The intense 957–977 cm^{-1} band appearing in all the W/Al–Ti(x) catalysts (Fig. 4) has been

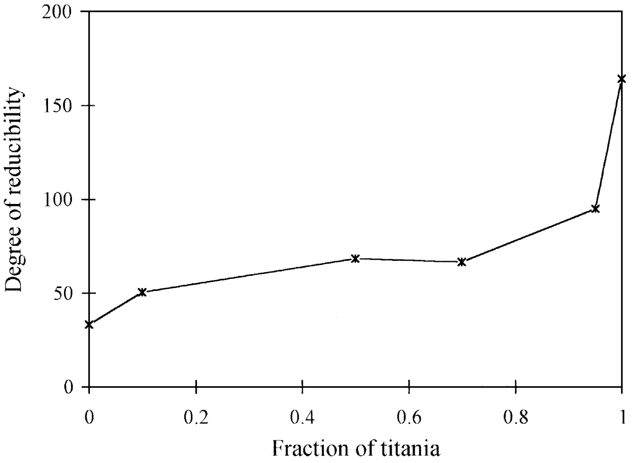

FIG. 10. Degree of reducibility of the W/Al–Ti(x) oxidic catalyst precursors.

assigned to the symmetric stretching vibration mode of W=O bonds in two-dimensional tungsten species in interaction with the support. The shift observed in this band when the titanium loading is increased may be due to different degrees of hydration which will also be related to the level of lateral interaction and distortion of the oxotungsten species. Apparently, the interaction of the water molecules with the oxidic tungsten surface species increases the degree of disorder or changes the symmetry of the bonds affecting, therefore, the symmetric stretching vibrational mode in the W=O terminal bonds. A similar effect has been reported for alumina-supported tungsten catalysts when the tungsten loading is increased (44). In fact, the degree of hydration of the tungsten oxidic species and their tungsten loading are related since an increase in the concentration of tungsten species on the surface promotes increased lateral interactions which impede the hydration of the tungsten species. The results from our laboratory indicate that the coverage used in this work are below the monolayer and, therefore, according to the literature (32, 33), on pure alumina, we should expect in the dehydrated state only the presence of tetrahedral tungsten species, while under ambient conditions, where some hydration occurs, a shift in the Raman peaks would be observed due to the degree of hydration which also changes the degree of tungsten coordination. Indeed, we observe on the alumina support under TPR conditions, which can be considered as dehydrated, the presence of only one type of tetrahedral tungsten species, while in the Raman characterization which was taken under ambient conditions, a shift in the Raman peak corresponding to W=O vibrations of tungsten surface species in interaction with the support is observed for the different samples.

The existence of a highly dispersed crystalline WO_3 phase in some of the samples seems also possible due to the presence of the weak band in 803 cm^{-1} characteristic of this species. However, as was mentioned before, the titania (anatase phase) presents also a weak band in ∼798 cm^{-1}, and therefore, the small increase observed in the 803 cm^{-1} band as the titanium content was raised may be also the result of an increased contribution of the ∼798 cm^{-1} anatase band.

In order to resolve the question if crystalline WO_3 was formed in our catalysts, and also if the shift observed in the ∼967 cm^{-1} band was due to an increased lateral interaction of the tungsten species, Raman analysis was made on an additional series of titania supported tungsten catalysts ($W(y)/TiO_2$, where $y = 1.4$, 2.8, 3.5, and 4.2 W atoms/nm^2) prepared using a commercial high-surface TiO_2 support (TiO_2 DT51 Rhone Poulenc, $Sg = 90$ m^2/g). The reason for using a TiO_2 support with higher surface area is to amplify the tungsten signal per gram of catalyst. These additional experiments will also allow us to determine at which loading the tungsten oxide monolayer is exceeded in WO_3/TiO_2-supported catalysts, since previous works (32) have stated the monolayer at the point where the appearance of WO_3 is clearly detected by Raman spectroscopy.

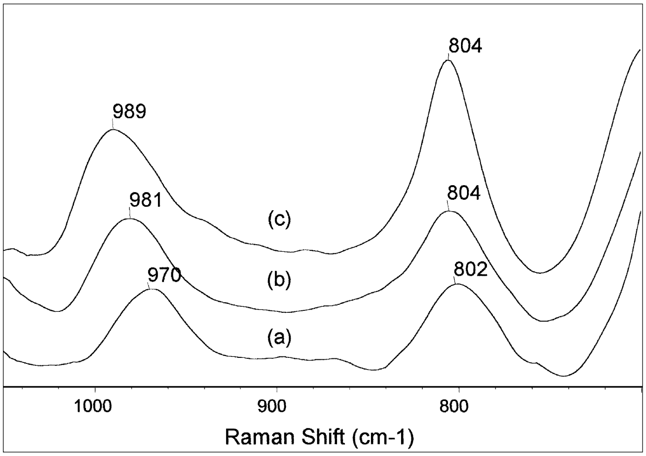

FIG. 11. FT-Raman spectra of tungsten catalysts supported on commercial TiO_2 (DT51 Rhone Poulanc, $S_{BET} = 90$ m^2/g), at different tungsten loading. (a) 1.4, (b) 2.8, and (c) 4.2 W atoms per square nanometer.

The Raman spectra of the W/TiO_2 catalysts with different tungsten loading (Fig. 11) shows that the 803 cm^{-1} band only increases significantly when the tungsten loading exceeds 2.8 W atoms/nm^2 indicating that the band observed at 1.4 and 2.8 W atoms/nm^2 loadings was mainly due to anatase. This result also indicates that for this support, the monolayer coverage for W/TiO_2 catalysts is between 2.8 and 3.5 W atoms/nm^2, which in our case are equivalent to 8.84 and 10.8 wt% WO_3. This result is fair agreement with the one reported by Vuurman *et al.* in Ref. (30) which corresponds to 3.7 W atoms/nm^2. A value of 4.2 W atoms per square nanometer has also been reported recently (33). According to these results, in our W/Al–Ti(x) catalysts with a tungsten loading of 2.8 W atoms/nm^2, the band appearing at 803 cm^{-1}, and which increases with the titania loading, may be assigned to an anatase contribution rather than to the presence of WO_3 crystallites.

Regarding the behavior of the band appearing at about ∼967 cm^{-1}, it is observed that in the $W(y)/TiO_2$ catalysts this band shifts from 971 to 985 cm^{-1} when going from the low ($y = 1.4$) to the high ($y = 4.2$) tungsten loading. This result indicates that the shift in this band, observed in the W/Al–Ti(x) catalysts when the titania content was varied from pure alumina to pure titania may well be due to an increased lateral interaction of the tungsten species. This increased lateral interaction will also be promoted by the diminished interaction of the tungsten oxidic phases with the support as the titanium loading is increased.

In line with the above results, the HREM observations in the sulfided samples indicate that the WS_2 crystallites in the W/Al–Ti(1.0) sample tend to growth laterally and to wrap the TiO_2 particles in contrast to the randomly distributed and smaller crystallites observed in the W/Al–Ti(0.0) catalyst.

The above findings are also in fair agreement with the idea proposed previously (33) that the net pH at ZPC of the support influences the structure of the hydrated surface species. In our case, the ZPC for alumina and titania are 8.5–9 and 6.0, respectively. Therefore, preferentially tetrahedral tungsten species will be expected to be present on pure alumina and octahedral tungsten species will be predominant on pure titania. The ZPC of the mixed oxides would be in an intermediate value and therefore a less clear definition in the coordination of the tungsten surface species would be expected. In line with this, our results from DRS and TPR clearly indicate a shift from tetrahedral to octahedral tungsten species when the support changes from pure alumina to pure titania. Furthermore, the appearance of DRS bands in the range ($\lambda = 290$–330 nm) for the samples with low titania contents ($x = 0.1$, 0.5, 0.7) at wavelengths which do not correspond either to a tetrahedral (~275 nm) coordination nor to an octahedral one, seems to point to the possible existence of pentahedral coordinated tungsten species. To this respect it has been proposed previously (27) in a XANES study of tungsten catalysts supported on titania, that the supported tungsten oxide consists of branched chains of pentahedral WO_5 units and terminal tetrahedral WO_4 units anchored onto the titania surface via W–O–Ti bonds. The length of these WO_5 units chains and thus the WO_4/WO_5 ratio being determined by the degree of tungsten oxide coverage and in our case also by the level of interaction of the tungsten species with the support. It was proposed by the same authors (27) that on adsorption of water, the oxygen coordination increases to six for all the surface tungsten sites. Furthermore, Kim *et al.* (32) has also suggested a different degree of polymerization of the tungsten oxide species on different supports.

The IR spectra of the oxidic samples also shows a shift in the band position of the W=O terminal bonds toward higher wavelengths with the titania loading. Thus, this band which in the alumina supported catalysts appears at 963 cm^{-1}, in those supported on titania appears at 993 cm^{-1} in agreement with the Raman results.

The results from this study allow us to propose a model for the different surface tungsten oxidic species when the formulation of the support is changed from pure alumina to pure titania going through a series of mixed oxides. A schematic representation of this model is presented in Fig. 12.

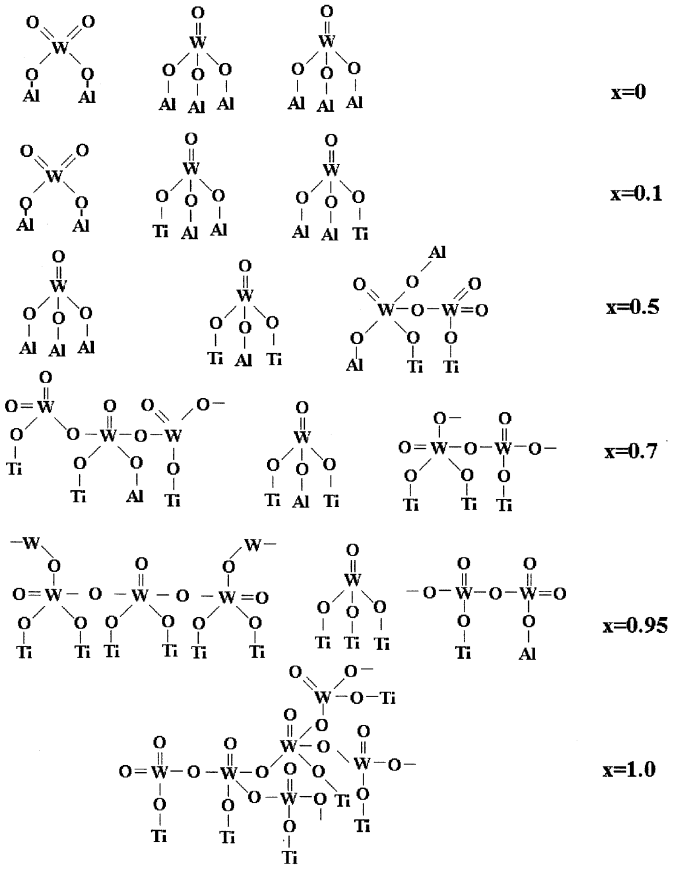

FIG. 12. Schematic model of the possible oxotungsten surface species present in the different W/Al–Ti(x) catalyst formulations.

Clearly, apart from the influence that the different tungsten precursor species will have on the catalytic activity, this will be influenced by the nature of the support since in this case the alumina support does not undergo reduction under reaction or sulfidation conditions, whereas the titania support does. Under reaction conditions these differences in the state of the supports will be expected to affect the number of tungsten coordinatively unsaturated sites present in the sulfided catalysts since the level of the so-called spill over of hydrogen (45), which has been proposed to have a bearing in the HDS reaction mechanism, will be affected by the presence of a sulfided titanium phase. The significant difference in activity between the pure titania-supported catalysts and all the other samples may well be related to this fact. Results from our laboratory indicate that the presence of the sulfided surface layer of titania plays a role in the reaction mechanism and induces higher activity, and that some vacancies created in this layer are capable of adsorbing NO (46). It should be interesting to undertake a detailed bulk and surface characterization study of rich titania Al_2O_3–TiO_2 samples to inquire more on the causes for the drastic changes in hydrodesulfurization activity observed in the rich titanium side of the support formulation.

From all the above results one may say that in the series of catalysts studied here the activity trend with titania loading is the result of the contribution of several effects which are interrelated. First, the change in the nature of the mixed oxide Al_2O_3–TiO_2 support with the titania loading promotes a change in the oxidic tungsten precursor species from tetrahedral to octahedral coordination. This change seems to be accompanied by the formation of oxopolytungstates. Second, the incorporation of titania to the alumina support results in a change in the level of interaction between the support and the tungsten phases in both the oxidic and the sulfided state, which leads to more reducible and quite possibly more sulfidable tungsten species. Third, the titania rich catalysts seem to lead to well dispersed oxidic tungsten species which promote slightly large WS_2 crystallites than for alumina but with a low level of stacking.

Finally, it is also quite possible that the drastic increase in activity observed for the pure titania supported catalyst may be also due to the role that the sulfided titania surface plays in the reaction mechanism in which quite possibly acts as a promoter.

CONCLUSIONS

From all the above results, the following conclusions can be drawn:

1. In the Al–Ti(x) supports, it is only at the high titania loading above $x = 0.7$ that anatase segregates forming crystallites detectable by XRD.

2. The support composition and physicochemical properties, determine the type of oxotungsten species present on the surface, leading to a gradual change from tetrahedral species present on alumina to octahedral species present on titania.

3. The degree of reducibility of the oxotungsten species seems to be a consequence of the level of interaction with the support and also, possibly, to the role of the reduced or sulfided layer of titanium present on the surface.

4. The presence of titania in the support seems to lead to oxotungstate species with greater lateral interaction which affect the size and the level of stacking of the WS_2 crystallites in the rich titania catalysts.

5. The observed changes in catalytic activity seem to be the result of changes in the interaction between the surface tungsten species and the support which leads to different surface species on the oxidic precursors and these in turn lead to a different morphology and quite possibly, different levels of sulfidation in the final sulfided tungsten species. It is quite possible that the enhanced activity of the titania supported catalyst is due to the role that the sulfided layer of titania plays in the mechanism of the HDS reaction, since no drastic change in the nature of the tungsten surface species either in the oxidic or sulfided state can account for the observed sharp increase in activity present in the pure titania supported sample.

ACKNOWLEDGMENTS

The financial support from PEMEX-Refinación and DGAPA-UNAM is gratefully acknowledged.

REFERENCES

1. Ramírez, J., Fuentes, S., Díaz, G., Vrinat, M., Breysse, M., and Lacroix, M., *Appl. Catal.* **52**, 211 (1989).
2. Thomas, R., De Beer, V. H. J., and Moulijn, J. A., *Bull. Soc. Chim. Belg.* **90**, 1349 (1981).
3. Chappell, P. J. C., Kibel, M. H., and Baker, B. G., *J. Catal.* **110**, 139–149 (1988).
4. Salvati, L., Makovsky, L. E., Stencel, J. M., Brown, F. R., and Hercules, D. M., *J. Phys. Chem.* **85**, 3700 (1981).
5. Chan, S. S., Wachs, I. E., Murrell, L. L., and Dispenziere, N. C., Jr., *J. Catal.* **92**, 1 (1985).
6. Grunert, W., Shpiro, E. S., Feldhaus, R., Anders, K., Antoshin, G. V., and Minachev, K. H. M., *J. Catal.* **107**, 522 (1987).
7. Breysse, M., *et al.*, *Catal. Today* **4**, 39 (1988).
8. Grimblot, J., Gengembre, L., and D'Huysser, A., *J. Electron. Spectrosc. Related Phenom.* **52**, 485 (1990).
9. López-Agudo, A., Benítez-Patricio, A., Ramírez Solís, J. F., and Vázquez, A., "13th North American Meeting of the Catalysis Society, Pittsburgh, PA, 1993," Abstract B-42.
10. Zhaobin, W., Qin, X., Xiexian, G., Grange, P., and Delmon, B., *Appl. Catal.* **75**, 179 (1991).
11. Ramírez, J., Ruiz-Ramírez, L., Cedeño, L., Harle, V., Vrinat, M., and Breysse, M., *Appl. Catal.* **93**, 163 (1993).
12. Iannibello, A., Villa, P. L., and Marengo, S., *Gazz. Chim. Ital.* **109**, 150–1 (1979).
13. Tittarelli, P., Iannibello, A., and Villa, P. L., *J. Solid State Chem.* **37**, 95 (1981).
14. Wachs, I. E., Chersich, C. C., and Hardenbergh, J. H., *Appl. Catal.* **13**, 335 (1985).
15. Carver, J. C., Wachs, J. C., and Murrell, L. L., *J. Catal.* **100**, 500 (1986).
16. Horsley, J. A., Wachs, I. E., Brown, J. M., Via, G. H., and Hardcastle, F. D., *J. Phys. Chem.* **91**, 4014 (1987).
17. Vermaire, D., and Berge, P. V., *J. Catal.* **116**, 309 (1989).
18. Brady, R. L., Southmayd, D., Contescu, C., Zhang, R., and Schwarz, J. A., *J. Catal.* **129**, 195 (1991).
19. Payen, E., Hubaut, R., Kasztelan, S., Poulet, O., and Grimblot, J., *J. Catal.* **147**, 123 (1994).
20. Zhang, R., Jagiello, J., Hu, J. F., Huang, Z. Q., and Schwarz, J. A., *Appl. Catal.* **84**, 123 (1992).
21. Stencel, J. M., Makovsky, L. E., Diehl, J. R., and Sarkus, T., *J. Raman Spectrosc.* **15**, 282 (1984).
22. Chan, S. S., Wachs, I. E., and Murrell, L. L., *J. Catal.* **90**, 150 (1984).
23. Thomas, R., Kerkhof, F. P., Moulijn, M., Medema, J., and De Beer, V. H., *J. Catal.* **61**, 559 (1980).
24. Murrell, L. L., Grenoble, D. C., Baker, R., Prestidge, E. B., Fung, S. C., Chianelli, R. R., and Cramer, S. P., *J. Catal.* **79**, 203 (1983).
25. Engweiler, J., Wharf, J., and Baker, A., *J. Catal.* **159**, 259 (1996).
26. Can, S. S., Watches, I. E., Mural, L. L., Wang, L., and Hall, W. K., *J. Phys. Chem.* **88**, 5831 (1984).
27. Hilbrig, F., Göbel, H. E., Knözinger, H., Schmelz, H., and Lengeler, B., *J. Phys. Chem.* **95**, 6973 (1991).
28. Scheffer, B., Molhock, P., and Moulijn, J. A., *Appl. Catal.* **46**, 11 (1989).
29. Ramis, G., Busca, G., Cristiani, C., Lietti, L., Forzatti, P., and Bregani, F., *Langmuir* **8**, 1744 (1992).
30. Vuurman, M. A., Wachs, I. E., and Hirt, A. M., *J. Phys. Chem.* **95**, 9928 (1991).
31. Deo, G., and Wachs, I. E., *J. Phys. Chem.* **95**, 5889 (1991).
32. Kim, D. S., Ostromecki, M., and Wachs, I. E., *J. Mol. Catal.* **106**, 93 (1996).
33. Wachs, I. E., *Catal. Today* **27**, 437 (1996).
34. Arnoldy, P., Jonge, J. C., and Moulijn, J. A., *J. Phys. Chem.* **89**, 4517 (1985).
35. Scheffer, B., Heijeinga, J. J., and Moulijn, J. A., *J. Phys. Chem.* **91**, 4752 (1987).

36. "Handbook of X-Ray photoelectron Spectroscopy" (C. D. Wagner, W. M. Riggs, L. E. Davis, J. F. Moudler, and G. E. Muilenberg, Eds.), p. 50, 68. Perkin–Elmer, 1978.
37. Stencel, M. J., "Raman Spectroscopy for Catalysis" (De. Burtron Davis, Eds.), p. 66. Van Nostrand Reinhold, New York, 1989.
38. Busca, G., Ramis, G., Gallardo, J. M., Sánchez, E., and Piaggio, P., *J. Chem. Soc., Faraday Trans.* **90**, 3181 (1994).
39. Yi, L., Ramis, G., Busca, G., and Lorenzelli, V., *J. Mater. Chem.* **4**, 1755 (1994).
40. Mangnus, P. J., Bos, A., and Moulijn, J. A., *J. Catal.* **146**, 437 (1994).
41. Zaikovski, L. M., Plyasova, M., Burmistrov, V. A., Startsev, A. N., and Yermakov, *Appl. Catal.* **11**, 15 (1984).
42. Vrinat, M., Breysse, M., Geantet, C., Ramírez, J., and Massoth, F., *Catal. Letters* **26**, 25 (1994).
43. Ramírez, J., Castillo, P., Benítez, A., Vázquez, A., Acosta, D., and López-Agudo, A., *J. Catal.* **158**, 181 (1996).
44. Wachs, I. E., Hardcastle, D. F., and Chan, S. S., *Spectroscopy* **1** (1986).
45. Delmon, B., *Stud. Surf. Sci. Catal.* **53**, 1 (1989).
46. Ramírez, J., and Gutiérrez-Alejandre, A., unpublished results.